Analysing a phase-frequency lock of a laser to an optical frequency comb

Maximilian Ammenwerth

Bachelorarbeit in Physik
angefertigt im Institut für Angewandte Physik

vorgelegt der
Mathematisch-Naturwissenschaftlichen Fakultät
der
Rheinischen Friedrich-Wilhelms-Universität
Bonn

August 2017

Ich versichere, dass ich diese Arbeit selbstständig verfasst und keine anderen als die angegebenen Quellen und Hilfsmittel benutzt sowie die Zitate kenntlich gemacht habe.

Bonn, ...

Datum Unterschrift

1. Gutachter: Prof. Dr. Dieter Meschede
2. Gutachter: Dr. Wolfgang Alt

Acknowledgements

Firstly I want to thank Prof. Dr. Dieter Meschede for giving me the opportunity to accomplish this Bachelor thesis within his research group. I learned a lot about laser operation and their stabilization onto other lasers, i.e. onto an optical frequency comb. The lab work and the daily discussions gave me a first insight to the fascinating field of quantum optics.

This project would not have been possible without the detailed explanations and instructions from my supervisor Dr. Deepak Pandey. I want to thank him for his assistance in the lab and the elucidating discussions of technical issues.

Special thanks goes to Tobias Macha for his patient help regarding all kinds of technical problems with the optical setup as well as the electronic setup. This project would not have reached the current status without his support.

Several electronic problems occurred during this project. I want to thank Dr. Wolfgang Alt for his detailed explanation of electronic issues and the help and guiding during the debugging process.

Furthermore I want to thank the whole group for their helpfulness and willingness for explanations and support at any time. I have been welcomed very warmly and I had an educational and funny time with them.

Finally special thanks goes to Lukas Ahlheit, since we were working together during this project. The cooperation was a lot of fun and also very productive. Specially during the beginning of this project we could clarify different thinks by discussing new learned topics. During the project we learned to foresee next steps and thus started working together efficiently.

Contents

CHAPTER 1

Introduction

In various experiments dealing with atomic physics, lasers with stable and well known frequencies are required [1]. In our research group an optical cavity has to be stabilized to a laser operating at 770 nm using the Pound-Drever-Hall technique [2]. The frequency of this laser has to be stabilized and should be scannable for several hundred MHz. This provides means of scanning the cavity resonance over atomic transitions. In order to stabilize the laser a stable reference is needed. Doppler-free saturated absorption spectroscopy can be used for example to stabilize a laser to an atomic transition [3], however, this scheme relies on the availability of an atomic transition at the desired wavelength. If this is not given, one might stabilize a laser to another laser which is then locked to an atomic transition. Therefore, a beat signal is created between both laser beams and measured with a fast photo diode [1, 4, 5]. The frequency difference between the laser beams has to lie within the bandwidth of the photo diode which effectively limits the frequency around the atomic transition accessible for stabilization. If the stability of one laser should be transferred over more than a few tens of GHz, one has to introduce other optical elements, like a transfer cavity.

In 2005, the Nobel Prize in Physics was awarded partially for the development of an optical frequency comb [6] . The frequency spectrum of such a comb consists of equally spaced components over a broad region of several tens of nm. The comb spectrum is stabilized using self referencing techniques which are explained in section 2.2. This Bachelor thesis describes the lock of an interference filter laser (IFL) to an optical frequency comb at 770 nm. In chapter 2 the idea of phase and frequency stabilization of one laser with respect to another laser is explained and a setup is introduced that allows locking a laser onto a frequency comb. In chapter 3 different schemes for continuous frequency tuning of a phase-locked laser are explained. The advantages and drawbacks of these schemes are compared and the implementation of one of these schemes is described. Chapter 4 deals with the characterization of the lock stability. A technique is introduced that allows a detailed analysis and verification of certain frequency modulations applied to the laser.

CHAPTER **2**

Phase-frequency stabilization

This chapter presents an overview of the techniques used for frequency stabilization. At first the idea of phase-frequency stabilization is explained. Secondly, stabilization to a frequency comb is briefly described and the optical and electronic setup is explained in detail. Finally the phase frequency discriminator (PFD) is described step-by-step.

2.1 Detecting phase and frequency drifts

In order to stabilize the frequency and phase of a laser, one has to measure the drifts of these values to apply proper feedback to the laser for bringing them back to the set point. Since optical frequencies are of the order of hundreds of THz one can not measure them directly with a photo diode. Alternatively it is common to create a beat between the laser and some stable optical reference. Due to interference, the intensity has a constant background plus an oscillating signal whose frequency depends solely on the frequency difference of the two laser beams, as shown in equation (2.1). If the optical reference is much more stable than the laser, fluctuations of the beat frequency are caused by fluctuations of the laser frequency.

$$\begin{aligned} E &= E_1 \cdot \exp(i\omega_1 t) + E_2 \cdot \exp(i\omega_2 t) \\ I \propto |E|^2 &= |E_1|^2 + |E_2|^2 + E_1 E_2^* \exp(i(\omega_1 - \omega_2)t) + E_1^* E_2 \exp(i(\omega_2 - \omega_1)t) \end{aligned} \tag{2.1}$$

For a phase-frequency stabilization, the beat signal is electronically compared with a reference signal using an error-signal-circuit (ESC). The output of this ESC, called error signal, indicates whether the beat frequency and phase fit to the reference signal. Deviations from the reference are translated to a voltage which is (at least in some region) proportional to the deviation. Many different ESCs have been developed, e.g. a RF interferometer [1], an electronic high pass circuit [4] or a frequency counter approach [5]. For this thesis, a phase-frequency discriminator (PFD) was used whose working principle is explained in section 2.6. The error signal is further processed in order to apply feedback to the piezo inside the laser and to the diode current. For this project a frequency comb (`Menlo Systems, FC1500-250-ULN`) is used as stable reference.

2.2 Optical frequency comb

An optical frequency comb provides a broad spectrum of equally spaced comb lines. This spectrum is generated by a femto-second pulsed mode locked laser. The working principle of a frequency comb can

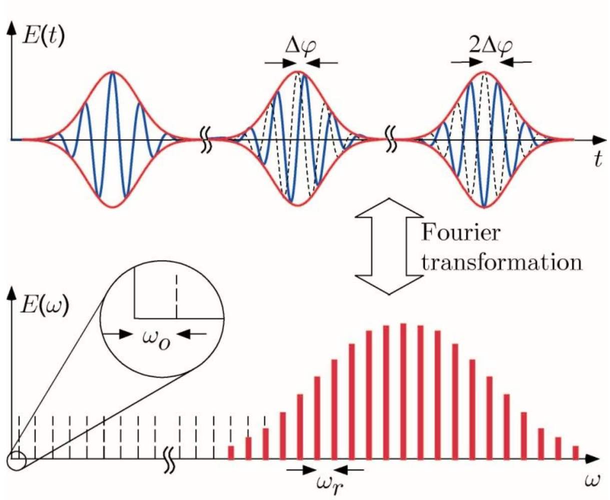

Figure 2.1: Frequency comb spectrum. Figure taken from [7].

be understood by analyzing laser pulses propagating inside a cavity. Two pulses are separated by the round trip time T that is defined by the cavity length L and the mean group velocity v_g. The carrier wave propagates with its phase velocity v_{Ph} which is not equal to the mean group velocity due to dispersion. That means that the phase of the carrier changes with respect to the envelope by $\Delta\varphi$ for each pulse. From the fourier transformation of such a time-domain signal one can obtain the frequency spectrum of the laser which is given by (2.2).

$$f_{\text{comb}} = f_{\text{CEO}} + n \cdot f_{\text{REP}} \tag{2.2}$$

Here n is an integer number which means, that comb lines are equally separated by the repetition rate frequency f_{REP}. The repetition rate frequency is the inverse round trip time and thus can be controlled by changing the cavity length. The repetition rate is directly measured with a photo diode that detects the pulse frequency of the comb laser. The carrier envelope offset frequency f_{CEO} occurs due to the phase shift $\Delta\varphi$ of the carrier between one pulse and the next one. This frequency is given by $f_{\text{CEO}} = \frac{\Delta\varphi}{2\pi \cdot T}$ and is measured by a f-$2f$-interferometer. A f-$2f$ interferometer exploits self-phase modulation in a highly non-linear fiber creating an octave spanning spectrum. Part of the spectrum is frequency doubled and recombined with the original spectrum allowing for the creation of a beat frequency. The corresponding beat frequency is shown in equation (2.3). The cavity envelope offset frequency is controlled via temperature control and an intra cavity electro optical modulator. More information about the comb can be found in the manual [7].

$$2 \cdot (f_{\text{CEO}} + n \cdot f_{\text{REP}}) - (f_{\text{CEO}} + 2n \cdot f_{\text{REP}}) = f_{\text{CEO}} \tag{2.3}$$

2.3 Stabilization to an optical frequency comb

In the previous section it has been explained that the laser is locked by beating it with the stable frequency comb light and comparing the beat signal with a stable RF reference. Equation 2.1 shows, that the beat frequency is given by the frequency difference between laser light and reference light. Since a frequency comb is used as reference light, the laser creates a beat with all the comb lines which means, that the beat signal includes multiple frequency components. First of all, a beat signal between the laser and the

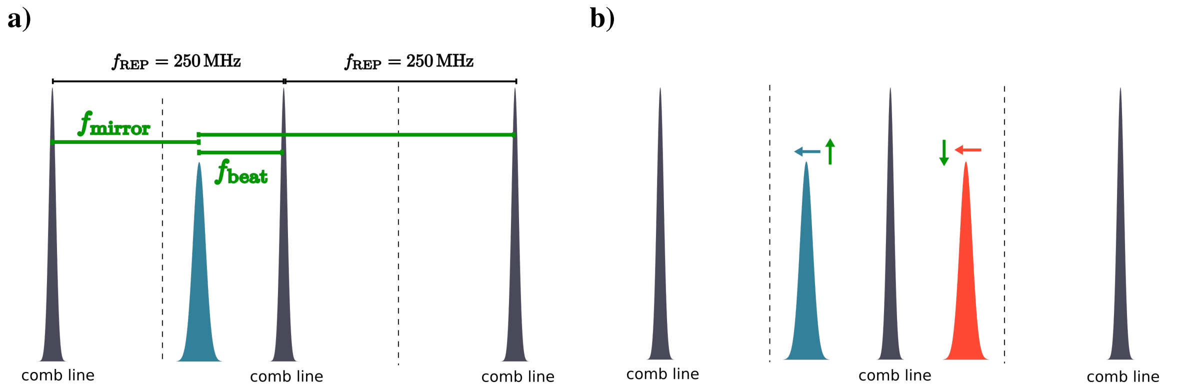

Figure 2.2: **a)** Since a beat is created between the laser and an optical frequency comb, each comb line is beating with the laser, so that the beat spectrum consists of multiple frequency components. The beat spectrum includes a beat between the laser and the comb line next to it, as well as a mirror beat with the other neighboring comb line. Additionally the other frequency components are given by the repetition rate frequency f_{REP} and the beat with other comb lines. Since the beat signal is analyzed by the PFD in time domain it is necessary to suppress frequencies higher than $\frac{f_{\text{REP}}}{2}$. **b)** In the beat detection unit the frequency difference between laser frequency and the nearest line is measured. The sign of this difference is unknown. If the frequency is lower than the frequency of the nearest line, the lock point lies on the left side of this comb line. Otherwise it lies on the right side. Assuming that the laser frequency decreases for both cases one observes that the beat frequency increases if the lock point lies on the left side. On the other hand the beat frequency decreases if the lock point lies on the right. Since the feedback has to compensate for deviations it is only possible to lock from one fixed side without inverting the feedback.

comb line next to it is created. The frequency of the corresponding beat can take values $f_{\text{beat}} \in \left[0, \frac{f_{\text{REP}}}{2}\right]$. Additionally a beat between the laser and the other neighboring comb line is created. The frequency of this "mirror beat" is given by $f_{\text{mirror}} = f_{\text{REP}} - f_{\text{beat}}$. Higher frequency components of the beat signal are given by the repetition rate frequency and beating with other comb lines. This is visualized in figure 2.2(a). The beat signal is further processed by the PFD which is processing the signal in time domain, which means that frequency components higher that $\frac{f_{\text{REP}}}{2}$ have to be suppressed. Since the beat frequency f_{beat} and, the mirror frequency f_{mirror} are moving symmetrically around $\frac{f_{\text{REP}}}{2}$, a sharp low pass filter with a cutoff exactly at $\frac{f_{\text{REP}}}{2}$ is needed, in order to have a broad bandwidth available for stabilization. The filter used in this thesis is described in [8].

2.3.1 Polarity of the lock point

The position of the laser frequency with respect to the nearest comb line is known as "lock point", since the laser frequency is stabilized to this value. If the laser frequency is lower than the nearest comb line, the lock point lies on the left side of the comb line. If it is higher the lock point lies on the right side of the comb line. Assuming that the laser frequency decreases for both cases, one observes an increasing beat frequency if the lock point lies on the left side. On the other hand, the beat frequency decreases if the lock point lies on the right. This is illustrated in figure 2.2(b). The electronic feedback circuitry can not distinguish between both cases since only the beat frequency is measured while the polarity is not detectable. Since the feedback has to compensate for deviations, it is only possible to lock from one fixed side without inverting the feedback. For this thesis the polarity was chosen such that the lock point lies on the left side of a comb line. The polarity can be easily inverted by exchanging the two inputs of the PFD.

2.4 Optical Setup

The optical setup used for beat detection is shown in figure 2.3. The laser is firstly coupled into a fiber in order to make a replacement of the laser easier if necessary. The light is then split with a polarizing beam splitter (PBS), and send into two separate arms. The PBS reflects or transmits the light depending on its polarization. By rotating the polarization of the incoming laser beam with a half wave plate (HWP), it is possible to adjust the power ratio between the two arms. Both arms consists of an acusto optical modulator (AOM) in double pass configuration. Inside the AOM a piezo driven by a radio frequency (RF) modulates density fluctuations in a crystal. The density wave travels through the crystal and creates a moving grating. The laser frequency is thereby effectively shifted by the applied radio frequency. The laser beam is retro reflected, after passing the AOM once and thus it passes the AOM again. Hereby a frequency shift of two times the AOM driving frequency is achieved. AOM 1 shifts the frequency of the light that is used for beat detection. AOM 2 shifts the light that is send to the experiment and is also used for intensity stabilization. For further description the two arms will be denoted "beat arm" and "experiment arm", respectively. The light in the beat arm is superimposed with the comb light for beat detection. A grating is used to filter out the part of the comb spectrum that is close to 770 nm.

2.5 Electronic Setup

The electronic setup is shown in figure 2.4. A DC-block (DCB) is used to remove the DC part from the photo diode signal. A high pass filter (HPF) and a low pass filter (LPF) are used to shape the beat signal. The LPF shows a sharp cutoff at 120 MHz. The purpose of this filter is to suppress frequencies higher than $\frac{f_{\mathrm{REP}}}{2} = 125\,\mathrm{MHz}$. The HPF is used for supporting the DC-block and has a cutoff frequency of 20 MHz. The filter design is explained in detail in [8]. A power splitter (PS) divides the signal so that one part can be monitored with a spectrum analyzer, while the other part is send to the PFD. The PFD compares the beat signal with the stable RF reference provided by a direct digital synthesizer (DDS) and provides two error signal outputs. The low frequency (LF) output is connected to a lock box in order to apply feedback to the piezo inside the laser. The high frequency output (HF) is connected to a loop filter, which then applies feedback to the diode current for phase locking. The reference frequency provided by the DDS (AD9954) is controlled by an mbed microcontroller (mbed LPC1768). The DDS is therefore programmed by the mbed via a serial peripheral interface (SPI). The driving frequency for AOM 1 is generated by a voltage controlled oscillator (VCO). This VCO is also controlled by the mbed via an analog line. The mbed controller itself has an analog input, which can be read out by arbitrary programs in order to control the setup. These programs are explained in [8].

2.5.1 Lock box

The lock box is used for frequency stabilization of the laser. It contains a PI controller, which processes the LF error signal. The output of such a PI controller consists of a proportional and an integral part as it is shown in equation (2.4).

$$c(t) = P \cdot e(t) + I \cdot \int_0^t e(\tau)d\tau \tag{2.4}$$

Here $e(t)$ denoted the LF error signal at time t. P and I are adjustable coefficients which control the proportional and integral gain of the controller. The output $c(t)$ is the signal that is sent to the piezo to correct the frequency deviations.

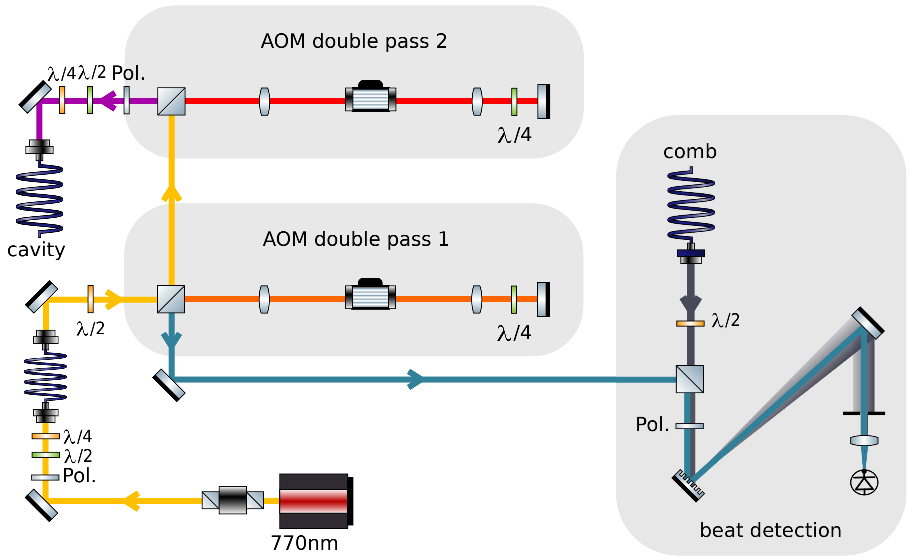

Figure 2.3: Optical setup consisting of the laser, two AOM double pass configurations and the beat detection unit. The light is firstly split into the two separate AOM double pass configurations which shift the frequency of the light by an applied radio frequency. AOM 1 shifts the light that is used for beat detection. AOM 2 shifts the frequency of the light that is sent to the experiment and is also used for intensity stabilization. The optical frequency is illustrated using different colors. Yellow corresponds to the original laser frequency. Blue indicates a frequency shifted by AOM 1 and purple indicates a shift by AOM 2. In the beat detection unit the laser light is superimposed with the comb light. A grating is used to filter out the part of the comb spectrum that is close to 770 nm.

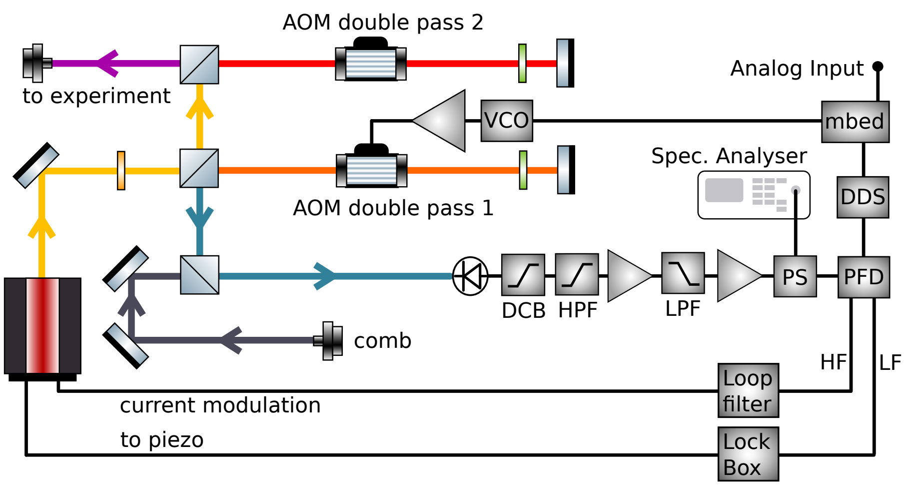

Figure 2.4: Simplified optical and electronic setup. The laser light is first shifted by AOM 1 and then superimposed with the comb light. The beat signal is detected with a fast photo diode. The output of the photo diode is amplified and shaped with multiple electronic filters. A power splitter sends part of the signal to a spectrum analyzer for monitoring purpose. The other half is connected to the PFD where it is compared to some stable reference provided by a DDS. The PFD provides two error signal outputs. The low frequency signal (LF) is connected to a lock box that applies feedback to the laser piezo. The high frequency signal (HF) is sent into a loop filter in order to apply feedback to the diode current. The driving frequency for AOM 1 is generated by a VCO that is controlled by an mbed microcontroller via an analog line. The mbed also controlles the frequency provided by the DDS. Therefore, the mbed and the DDS communicate via a serial peripheral interface.

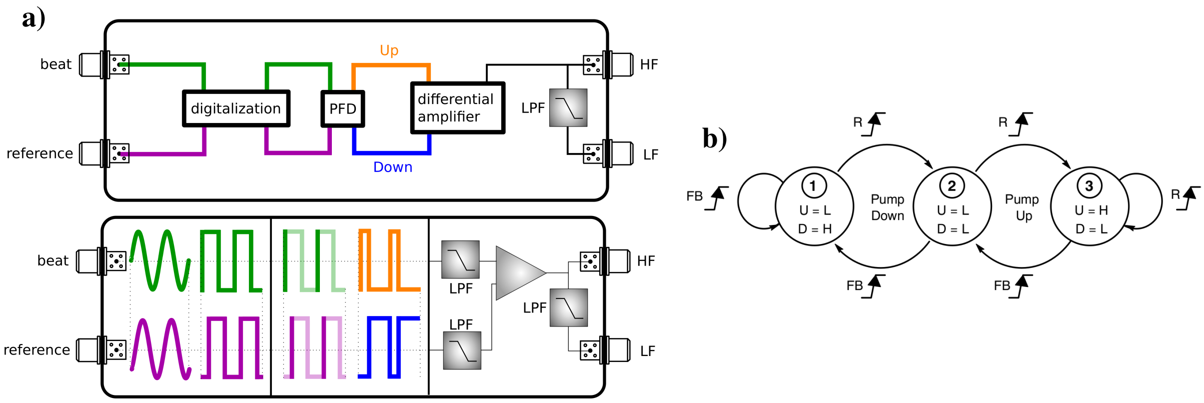

Figure 2.5: **a)** Schematic overview over the PFD. **b)** Logic diagram of the MC100EP140. One can see that the chip is sensitive to rising edges on the reference (R) and beat (FB) input. The two output signals up (U) and down (D) are either in the high (H) or the low (L) state and change between these states as shown. Figure taken from the data sheet of the MC100EP140 [9].

2.5.2 Loop filter

The loop filter consists of a low pass filter, a lead filter, a voltage divider and some protection circuitry. The low pass filter is used to filter frequencies that are to high for correction purposes. The leak filter shifts the phase of the signal to make sure that negative feedback is applied to the current modulation, such that phase deviations are suppressed and not amplified. A voltage divider is used to control the gain. Zener diodes and a DC blocking capacitor are inserted at the output of the loop filter to limit the current sent into the laser.

2.6 Phase frequency discriminator

In order to achieve a phase-frequency lock of an IFL, one has to apply proper feedback to the piezo and the diode current. This feedback has to compensate for deviations of the frequency and the phase. These deviations are detected and quantified by a PFD, that was developed by Professor Marco Prevedelli, Università di Bologna. The PFD circuitry can be divided into 3 parts. The sinusoidal input is first digitized by an AD96687 comparator. The digitized signals are then fed into the phase-frequency detector MC100EP140. This chip has two differential outputs whose behavior is described by the logic diagram in figure 2.5(b). The behavior of the differential “Up” and “Down” output is analyzed with two function generators, which were both locked to the 10 MHz reference signal from an atomic clock. The function generators were configured to have the same frequency but a phase difference. From the logic diagram one can see that in this case the PFD is oscillating between two states. Either between 1 and 2 or between 2 and 3. In both cases one of the differential outputs is fixed at its low level, while the other one is oscillating between high and low level. The duty cycle of this output corresponds to the phase difference of the input signals. This is shown in figure 2.6(a,b). The differential output signals of the MC100EP140 are then smoothed with a low pass filter, in order to convert the duty cycle to a DC voltage. The cutoff frequency of this first order low pass filter is at 33.9 MHz. The difference between the differential outputs after low pass filtering is then amplified with a AD8129 differential amplifier. The output of this amplifier serves as HF error signal. The LF error signal is derived from that by filtering with a first order low pass that has its cutoff frequency at 3.4 MHz. The PFD translates a phase difference into a proportional DC voltage. This voltage has boundaries which means, that for phase differences higher than some $\Delta\varphi_{\text{max}}$ the output voltage saturates. It follows from this that the "phase span" which can be covered by the PFD is smaller than 2π. Experimentally it turned out that the phase span of the PFD is of the order of 10 % of 2π.

2.6.1 RF leakage

In the previous section, it has been explained that the PFD stores the phase information in the duty cycle of two differential outputs. This duty cycle is then converted into a DC voltage by a low pass filter. If one wants to detect a phase difference for signals which have a frequency that is close to the cutoff frequency of the smoothing low pass, one observes "RF leakage". In this case the duty cycle is not converted properly to a DC voltage and the error signal is not constant although the phase difference is kept constant. This can be seen in figure 2.6(c). For a constant phase deviation between the two input signals of the PFD the error signal should be flat. If the error signal is affected by RF leakage, one can measure an oscillation of the error signal which is frequency dependent. The amplitude of the error signal oscillation is shown in figure 2.6(d) as function of frequency. By increasing the capacitance of the low pass filter, it is possible to reduce its cutoff frequency, since this is given by $f_{\text{cutoff}} = \frac{1}{2\pi RC}$. Here R is the resistance of the low pass and C the capacitance. Figure 2.6(d) shows that one can reduce the influence of RF leakage by changing the cutoff frequency of the smoothing low pass. Without additional capacitors it is possible to establish a stable phase lock for beat frequencies higher than 60 MHz. By adding a 22 pF capacitor to the existing 4.7 pF capacitor the cutoff frequency is changed to 6 MHz. With this changes it is possible to establish a stable phase lock for frequencies higher than 40 MHz. With additional capacitors, it is still not possible to lock at beat frequencies lower than 40 MHz, although the AC amplitude of the error signal is lower than the former limit at 60 MHz without additional capacitors. This cannot be explained with RF leakage and remains unknown. For further analysis one should lock at the frequency dependant amplification of the differential amplifier.

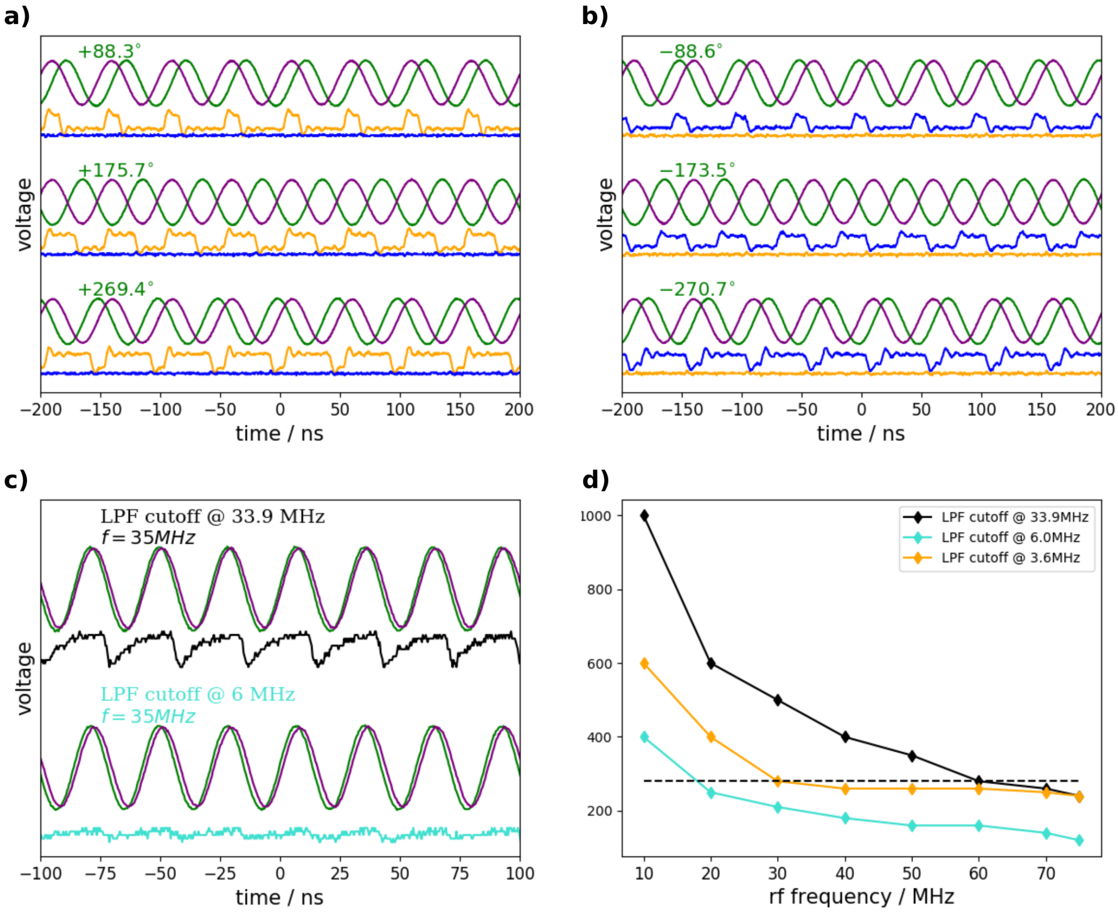

Figure 2.6: **a)+b)** Phase information is stored in the duty cycle of the differential outputs of the PFD. Two function generators (green,purple), both locked to the atomic clock, were configured to have the same frequency but a phase difference. One can see that the duty cycle of the differential up (yellow) and down (blue) output carries the phase information. The phase difference between 0 and 2π is proportionally mapped to a duty cycle between 0 and 1. **c)** RF leakage for different cutoff frequencies of the smoothing low pass filter. **d)** AC amplitude of the error signal as function of RF frequency for constant phase deviations. The AC amplitude is measured for different cutoff frequencies of the smoothing low pass filter. Without any additional capacitor it is possible to establish a stable phase lock for frequencies higher than 60 MHz. The dashed line indicates the AC amplitude of the error signal for this frequency without changing the cutoff of the low pass.

CHAPTER 3

Continuous frequency tuning of a phase-locked laser

This chapter is devoted to the techniques used for scanning the laser frequency continuously over several hundreds of MHz, requiring scanning across multiple comb lines [10–12]. This demands eloquent techniques while crossing a comb line in order to maintain phase stability of the lock. In this regard 3 different scanning schemes are explained and compared. The implementation of one of these schemes is described. All schemes have in common that the optical frequency of the locked laser is set in particular by the frequency difference between the laser frequency and the nearest comb line, since the beat signal of these is used for stabilization. For further description the relative position of the laser frequency with the respect to the nearest comb line is denoted as "lock point". The need of a lock point jump is explained within this chapter and the optimization of this process is described.

3.1 Moving the lock point

If the reference signal for the PFD is changed, an error signal is generated which indicates the deviation between beat frequency and its new set point. Feedback to the laser piezo and diode current is generated from this error signal by the lock box and the loop filter. This feedback changes the optical laser frequency such that the new beat frequency matches the reference frequency. Hereby the laser can be scanned. In the ideal case, the scannable bandwidth is given by $\frac{f_{\mathrm{REP}}}{2} = 125\,\mathrm{MHz}$. For beat frequencies close to $\frac{f_{\mathrm{REP}}}{2}$, the lock might be disturbed by the mirror beat, due to competition between beat frequency and mirror frequency. The maximum beat frequency is limited by the frequency response of the low pass filter. A sharp cutoff at $\frac{f_{\mathrm{REP}}}{2}$ is needed in order to allow locking at beat frequencies close to $\frac{f_{\mathrm{REP}}}{2}$. With the used low pass filter a stable lock is possible for frequencies up to 115 MHz. On the low frequency side one is limited by the ESC. Experimentally it turned out that the PFD is not working properly for frequencies lower than 40 MHz as described in section 2.6. A scannable bandwidth of 75 MHz is obtained from these boundaries. If the laser needs to be scanned over broader regions where locking is not directly possible due to the discussed issues, one has to insert a frequency shifting element either in the beat arm or the experiment arm. In this case the laser frequency at the output of the locking setup is shifted with respect to the lock point. Hereby it is possible to keep the lock point in the valid region while the output frequency can be tuned continuously.

3.2 Scanning schemes

For this project an AOM was used in double pass configuration such that the optical laser frequency is shifted by two times the AOM driving frequency. The setup includes a double pass in the beat arm (AOM 1) and the experiment arm (AOM 2) as it is shown in figure 2.4. Both AOMs are used in positive first order double pass and shift the laser frequency as shown in figure 3.1(a). With this configuration, different scanning schemes are possible which will be explained next. These schemes have their own advantages and drawbacks and are compared in this section.

3.2.1 AOM 1 based scanning

In this scheme, the driving frequency of AOM 1 is changed [11]. This causes a change of the optical frequency used for beat detection and consequently a change of the beat frequency. The deviation from the reference frequency causes feedback to the laser to bring the lock point back to the set point, such that the laser frequency is effectively scanned. By changing the frequency of AOM 1 it is possible to keep the lock point in the valid region while the laser frequency can be scanned continuously. The driving frequency of AOM 2 can be set to a constant value. It is then used for intensity stabilization only. If one wants to scan the laser frequency upwards, one can first reduce the reference frequency such that the lock point comes closer to the comb line. Since the lock point lies on the left side of a comb line, a reduction of the reference signal causes an increasing laser frequency. If the laser needs to be scanned further, one has to reduce the driving frequency of AOM 1. Since the lock point is fixed via the feedback the laser frequency is increased that way. Once the laser has been scanned for $f_{\mathrm{REP}} = 250\,\mathrm{MHz}$ one has to simultaneously reset the reference frequency f_{ref} and the AOM 1 driving frequency f_{aom1} such that the lock point jumps to the next comb line, preparing it for another round of action. During this jump the comb line used for beat detection changes but the optical output frequency remains constant. For a smooth jump of the lock point without disturbing the laser, one has to make sure that equation 3.1 holds.

$$\left(f_{\mathrm{ref,max}} - f_{\mathrm{ref,min}}\right) + 2 \cdot \left(f_{\mathrm{aom,max}} - f_{\mathrm{aom,min}}\right) = f_{\mathrm{REP}} \tag{3.1}$$

Here $f_{\mathrm{ref,min}}$ and $f_{\mathrm{aom,min}}$ denote the reference frequency and the AOM driving frequency before the lock point jump. The frequencies after the lock point jump are denoted by $f_{\mathrm{ref,max}}$ and $f_{\mathrm{aom,max}}$. This order changes if the laser frequency is scanned downwards. If equation (3.1) is not fulfilled precisely the laser frequency is changed during a jump of the lock point. For optimization of the jump it is possible to monitor the error signal during the jump. If the error signal remains flat, the laser frequency in the experiment arm is not changed independently of the processes in AOM 1. The lock point jump is explained in detail in section 3.3. The signals used for scanning the laser are shown in figure 3.1(b).

3.2.2 AOM 2 based scanning

In this scheme the driving frequency of AOM 1 is kept constant but the AOM 2 frequency is changed in order to scan the laser [10, 12]. The laser can be scanned again by changing the reference. In order to increase the laser frequency over the "forbidden region", one has to increase the driving frequency of AOM 2. The intensity stabilization is again done with AOM 2. The AOM in the beat arm is not used in this scheme. An advantage of this AOM 2 based scanning is that only one AOM is necessary for scanning and intensity stabilization. Scanning with AOM 2 is also faster since it does not dependent on the locking bandwidth. A serious drawback is that the output frequency of the setup is scanned continuously while the laser itself is not following continuously. That means that during the lock point jump the laser frequency has to be changed by $2 \cdot \left(f_{\mathrm{aom,max}} - f_{\mathrm{aom,min}}\right)$. This is shown in figure 3.1(c). The execution

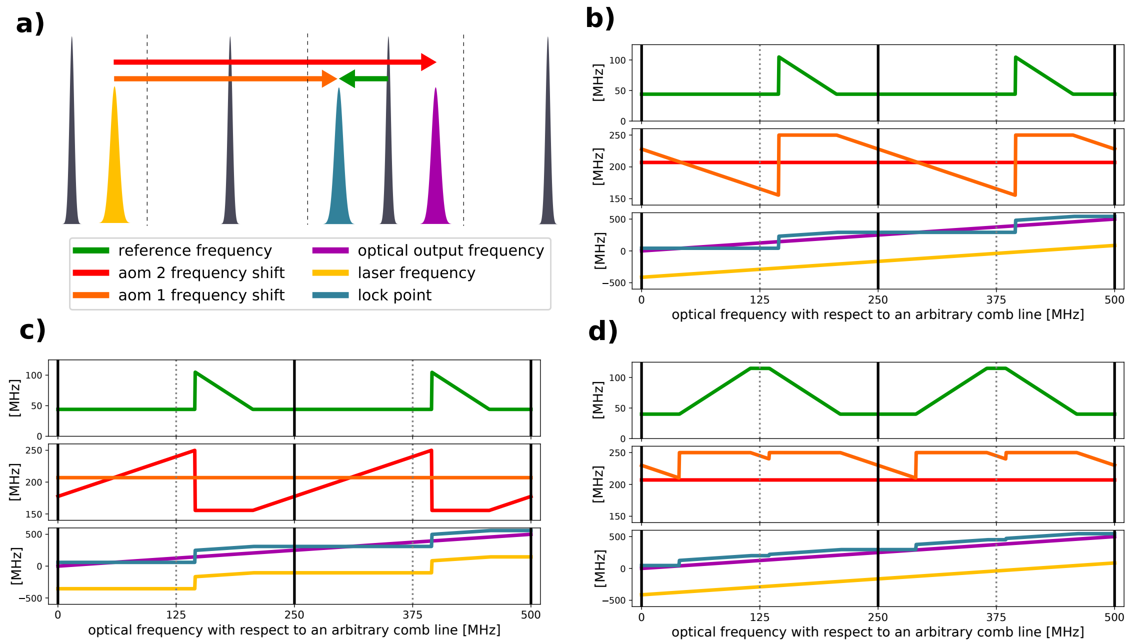

Figure 3.1: **a)** The laser light (yellow) is split and send into two separate AOM double pass configurations. AOM 1 (orange) shifts the light in the beat arm that is used as lock point (blue). AOM 2 (red) shifts the light in the experiment arm (purple). In the beat detection unit a beat signal is measured between the light in the beat arm and the frequency comb. This beat signal (green) is used for locking **b)** AOM 1 based scanning. The laser frequency is scanned by changing either the reference frequency or the driving frequency of AOM 1. AOM 2 is kept at a constant frequency and is used only for intensity stabilization. At some point the reference and the AOM 1 frequency have to be reset, so that the lock point jumps to the next comb line. **c)** AOM2 based scanning. The laser is scanned by changing the reference frequency or the AOM 2 driving frequency. **d)** Polarity change scheme. The laser can be locked from both sides to a comb line, since the polarity is inverted properly. Scanning the laser over comb lines includes an AOM in the beat arm.

time of such a frequency step of the laser frequency is limited by the bandwidth of the piezo inside the IFL. It follows, that a lock point jump in this scheme is slower and less stable, since the laser frequency has to follow the previous scan. The frequency step could be implemented by charging capacitors that are then "fired" into the laser[13]. Optimization of the jump in this scheme is more complicated since neither the beat signal nor the error signal can be used as feedback.

3.2.3 Polarity scheme

In this scheme the polarity of the feedback is invert-able such that the laser can be locked from both sides to a comb line. An AOM in either the beat arm or the experiment arm is nevertheless necessary because locking does not work close to comb lines and in the middle between two comb lines. In figure 3.1(c) an AOM in the beat arm is assumed. Two jumps per 250 MHz scan are needed, since the forbidden region next to comb lines have to be bypassed as well as the region close to the polarity change. The error signal can be used as feedback for optimizing the jump. For this project AOM 1 based scanning was implemented. An AOM in the experiment arm was also installed in order to make a intensity stabilization of the laser beam possible. This AOM 2 is also useful for faster "out of loop" tuning of the laser frequency. The only disadvantage of this setup is, that it binds more optical and electronic components.

3.3 Lockpoint jump

During the lock point jump the driving frequency of the AOM in the beat arm as well as the reference signal provided by the DDS is changed. This is shown in figure 3.2(a). The optical laser frequency should not be changed during this process. Therefore, it is important that the laser does not undergo feedback which would change the frequency or phase. Consequently, it is important that the error signal does not cause such a feedback. During the jump the optical frequency on the photo diode is changed due to the change of the AOM driving frequency. Consequently, the efficiency of the AOM is also changed during the AOM ramp [8]. Due to this efficiency ramp the optical power on the photo diode is changed which causes a change of the DC part of the photo diode signal. On the rising edge of the AOM efficiency the DC part of the photo diode signal increases. The derivative of the DC increase passes the DC block and causes the amplifiers to saturate so that no meaningful beat signal is obtained during the jump. This is shown in figure 3.3(b). It is therefore not possible to have active feedback on the laser within the "jumptime". In order to avoid disturbing the laser, it is necessary to adjust the reference frequency from the DDS in a way that the PFD generates a error signal with smallest possible amplitude.

The AOM driving frequency is generated by a VCO which is controlled via an analog output line of the mbed microcontroller. The analog line is amplified for technical reason. In order to fulfill equation 3.1, one has to precisely adjust the input value of the digital to analog converter such that the frequencies are generated properly. For this optimization process it is convenient to monitor the error signal during the jump. If the values are not properly set, one observes a saturation of the error signal which means that the laser frequency is changed. This can be seen in figure 3.2(b). By adjusting the frequencies of the reference signal and the AOM driving signal it was possible to reduce the time within the error signal saturates down to 13 µs. This short saturation occurred due to missing synchronization of the reference frequency jump and the AOM frequency jump. To synchronize the jump a certain frequency ramp is preprogrammed in the DDS board. This ramp is executed on a trigger event which allows a precise synchronization with the change of the AOM driving frequency. The frequency ramp includes a certain "waiting time", before changes are applied, in order to get the mbed enough time to change the AOM frequency. A schematic overview over the steps executed during the jump is shown in 3.2(c). During the jump the reference frequency is increased and decreased step wise in order to keep the error signal oscillating around zero. In figure 3.3(a) one can see a measurement of the error signal, the beat signal and the reference signal from the DDS during the lock point jump. The frequency of the reference signal is changed during the jump in order to keep the error signal as flat as possible.

3.4 Optical frequency synthesizer

The frequency comb spectrum consists of multiple equally spaced comb lines and thus provides a frequency ruler which can be used for synthesizing optical frequencies with high precision [14]. The optical laser frequency at the output of the locking setup is defined by the position of the lock point and the AOM frequencies. If the comb line number used for locking is known, it is possible to synthesize an arbitrary optical frequency by adjusting the reference frequency and the AOM frequencies. For this calibration procedure it is necessary to measure the optical frequency with a wavemeter. The comb line number n which is used for locking can then be calculated by formula (3.2). Therefore it is necessary that the optical frequency is known with a precision better than $\frac{f_{\mathrm{REP}}}{2} = 125\,\mathrm{MHz}$.

$$n \cdot f_{\mathrm{REP}} + f_{\mathrm{CEO}} = \underbrace{f_{\mathrm{out}} - 2 \cdot f_{\mathrm{aom2}} + 2 \cdot f_{\mathrm{aom1}}}_{\text{lock point}} + f_{\mathrm{beat}} \tag{3.2}$$

With a known lock point it is then possible to synthesize optical frequencies by adjusting the AOM driving frequencies and the reference frequency for the PFD. The accuracy of the synthesized optical frequency depends on the accuracy of the VCO and the DDS frequency. Since all this frequencies occur linear in formula (3.2) the uncertainties can be simply summed up taking the prefactor 2 into account. Note that the carrier envelope offset frequency f_{CEO} might be negative.

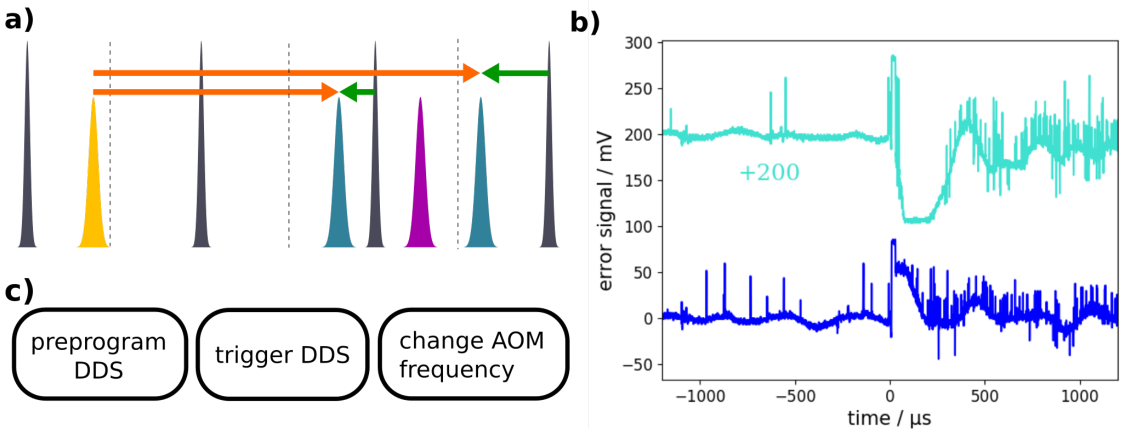

Figure 3.2: **a)** During the lock point jump the AOM driving frequency (orange) and the reference frequency (green) are changed. That causes the lock point (blue) to jump to the next comb line while the laser frequency (yellow) and the output frequency (purple) are not changed. **b)** Measurements of the error signal during the lock point jump. If the frequencies are not properly chosen such that equation 3.1 holds, one observes that the laser frequency is changed unintentionally, which can be seen on the error signal. **c)** Schematics of the program executed by the mbed controller during the lock point jump.

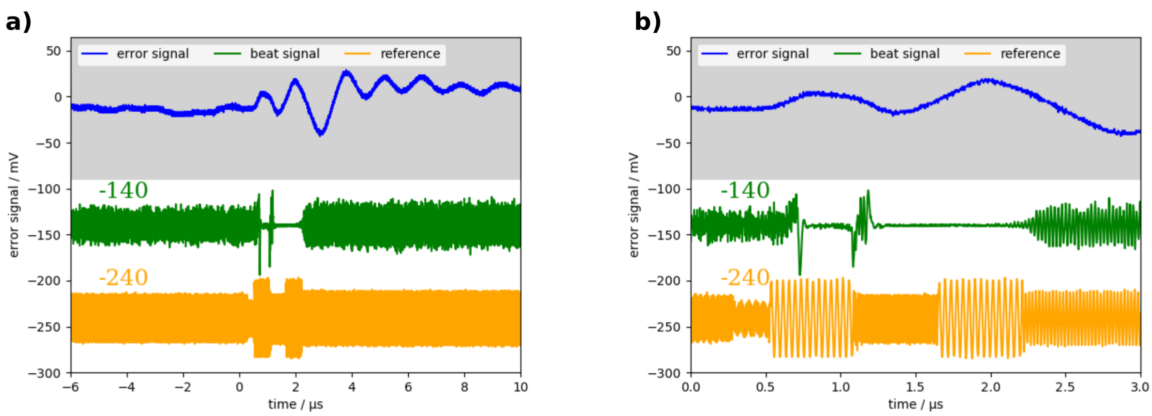

Figure 3.3: **a)** Measurement of the error signal (blue), the beat signal (green) and the reference signal (yellow) during the lock point jump. The beat signal vanishes during the jump due to a change in the AOM efficiency which causes the amplifiers to saturate. The reference signal from the DDS is adjusted in a way that the PFD generates an error signal with smallest possible amplitude in order to avoid a change of the optical laser frequency. The amplitude of the error signal is smaller that its saturation level, which is indicated by the grey box. **b)** Zoomed version of the same signals.

CHAPTER **4**

Analysing lock stability

For a quantitative study of the phase and frequency stability of a locked laser, one can use different techniques which analyze either electronic “in-loop signals” that are used for stabilization or “out of loop” signals that are not used for feedback generation. The coarse and long term frequency stability is analyzed with a wavemeter that records the optical frequency of the stabilized laser beam as function of time. The available frequency resolution is of the order of a few MHz, which is limited by the resolution of the wavemeter. When the laser is referenced to an optical frequency comb, a wavemeter measurement is useful to verify that the laser is always locked to the same predetermined comb line. If the comb line that is used as lock reference changes unintentionally, the wavemeter measures a frequency step of $f_{\mathrm{REP}} = 250\,\mathrm{MHz}$. The gain parameters of the servo lock loop are adjusted to avoid any unintended lock point jump due to external disturbances. Another intuitive way for in loop lock stability analysis would be to monitoring the error signal since this signal is quantifying phase and frequency deviations. The resolution of phase and frequency deviations in this case depends on the ESC and is usually very precise compared to the other possible measurements. Also the in-loop beat signal that is used for stabilization can be analyzed in terms of its power spectral density. This spectrum usually shows a typical feature of the central carrier peak at the desired lock point and two servo bumps also called sidebands. The control bandwidth can be estimated from the position of these sidebands with respect to the central carrier. The residual phase noise can be estimated from this spectrum by determining the power in the sidebands. For this project it is of interest to analyze the phase and frequency stability during the lock point jump and also during certain frequency ramps of the laser. Especially the phase and frequency stability during the lock point jump has to be verified. In order to analyze the lock point jump a wavemeter measurement is not useful, since the available wavemeter resolution is not precise enough. It is also not possible to use the error signal for a stability verifying analysis, since this signal was already used for optimization. In addition to that it is not possible to use the in-loop beat spectrum, due to the saturation of the amplifiers during the jump. Because of this saturation the beat signal is not meaningful during the jump, as it was explained in more detail in section 3.3. In order to analyze the stability of the phase and the frequency a more elaborated analysis is required. This analysis is based on another out of loop beat signal between the stabilized laser beam and the frequency comb. For an estimation of the frequency stability from this signal one has to measure the frequency and phase of the beat signal as function of time. This approach is described further in section 4.2.

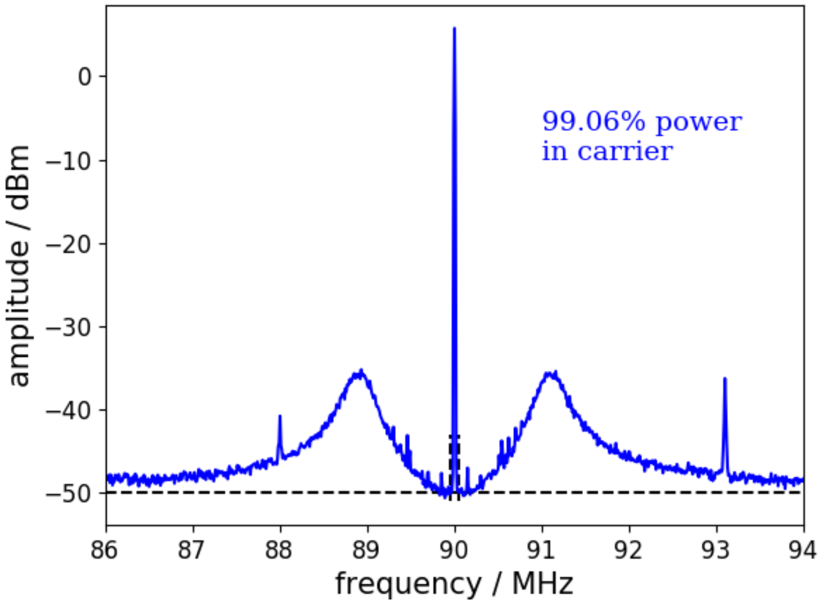

Figure 4.1: Beat signal measured with a spectrum analyzer while the laser was locked. The frequency resolution is set to 10 kHz and the spectrum is averaged over 10 traces. The central peak at 90 MHz is surrounded by two servo bumps at a relative position of ±1.1 MHz

4.1 In-loop beat signal

This section deals with the analysis of the beat signal that is used for locking. As shown in fiure 2.4 a power splitter divides the beat signal so that a spectrum can be measured with a spectrum analyzer while the laser is locked. A measured beat spectrum for this locked case is shown in figure 4.1. It is obtained that 99.06 % of the power lies inside the carrier peak. The carrier peak at exactly 90 MHz is surrounded by two servo bumps at a relative position of ±1.1 MHz. This frequency difference can be interpreted as locking bandwidth. The area under the servo bumps represents phase noise of the beat signal with respect to the central carrier peak.

4.2 Time frequency analysis

For further analysis of the phase and frequency stability one can take the stabilized laser beam and create another beat signal with the frequency comb. This second out-of-loop beat signal is not used for correction purpose and thus a more reliable out of loop analysis can be done by analyzing this beat signal. For this project the beat signal was measured in time domain with a 2.5 GS s^{-1} oscilloscope. Traces were recorded for a time span of 2 ms.

Assuming that the laser frequency is properly stabilized, a constant beat frequency is measured. Therefore it is important to obtain the beat frequency as function of time. In order do obtain the corresponding spectra one has to multiply the signal with a window function before calculating the Fourier spectrum. The window function is zero except for some region of interest, such that the time dependency can be analyzed by moving the window over the signal. The influence of the window function is explained in more detail in section 4.2.2.

4.2.1 Frequency resolution

The number of frequency bins returned from the FFT algorithm determines the resolution of the spectrum. This bin width Δf_{fft} can be calculated from the sampling rate f_{sample} and the number of data points N by equation (4.1).

$$\Delta f_{\text{fft}} = \frac{f_{\text{sample}}}{N} \tag{4.1}$$

In order to reduce the bin width "zero padding" can be used. This technique adds a series of zeros to the time domain signal such that the number of data points N is effectively increased. No frequency components of interest are appended, since only a DC part of frequency 0 Hz is added. In order to analyze the influence of zero padding a simulated signal was used consisting of two monochromatic sinusoidals with frequencies 50 MHz and 50.5 MHz. White noise with a σ of 10 % of the signal amplitude was added. Figure 4.2 shows the influence of zero padding for this signal. In 4.2(a) the signal shown in 4.2(d) is analyzed directly without adding zeros. In 4.2(b) zeros are added such that 50 % of the analyzed window contains zeros. In 4.2(c) the analyzed window contains 99 % zeros. One can see that the number of data points lying in the 10 MHz span increases. In spite of the small frequency bin width one does not see two clear peaks at the expected frequencies of 50 MHz and 50.5 MHz. Although the FFT resolution is good enough, the "signal resolution" Δf_{signal} is not. The signal resolution is according to equation (4.2) the inverse time span of the time domain data and represents the minimum detectable frequency difference.

$$\Delta f_{\text{signal}} = \frac{1}{T} \tag{4.2}$$

If the signal is not zero padded, the signal resolution Δf_{signal} and the frequency bin width Δf_{fft} are equal. Zero padding is useful to clarify the exact position of a maximum within a peak. Figures 4.2(d-f) show the influence of different window length. For spectrum 4.2(d) a 2 µs window was used, that was filled with zeros to reach a 200 µs span. For spectrum 4.2(e) 20 µs time domain data was used and 180 µs of zeros were added in order to have the same bin width as in 4.2(d). In 4.2(f) a 200 µs window was used and no zeros were added. For all these spectra the frequency bin width is 5 kHz, while the signal resolution changes between 500 kHz for 4.2(d), 50 kHz for 4.2(e) and 5 kHz for 4.2(f), respectively. From equation (4.2) it becomes clear, that the signal resolution can be improved by increasing the amount of time domain data used for each spectrum. One has to decide whether a good time or frequency resolution is necessary since the product of time uncertainty $\Delta t = T$ and frequency uncertainty Δf_{signal} is fixed, according to equation (4.3).

$$\Delta f_{\text{signal}} \cdot \Delta t = 1 \tag{4.3}$$

For this project a monochromatic frequency is expected and thus the maximum of the frequency distribution is of interest. The position of the maximum is independent of the width of the corresponding peak and thus the position of the maximum is mainly defined by the bin width and not be the signal resolution. Therefore it is possible to use a "fine" time resolution and increase the frequency resolution with zero padding. Different window functions can be used for analyzing the frequency dependence. There influence on the calculated spectrum is discussed in the next section.

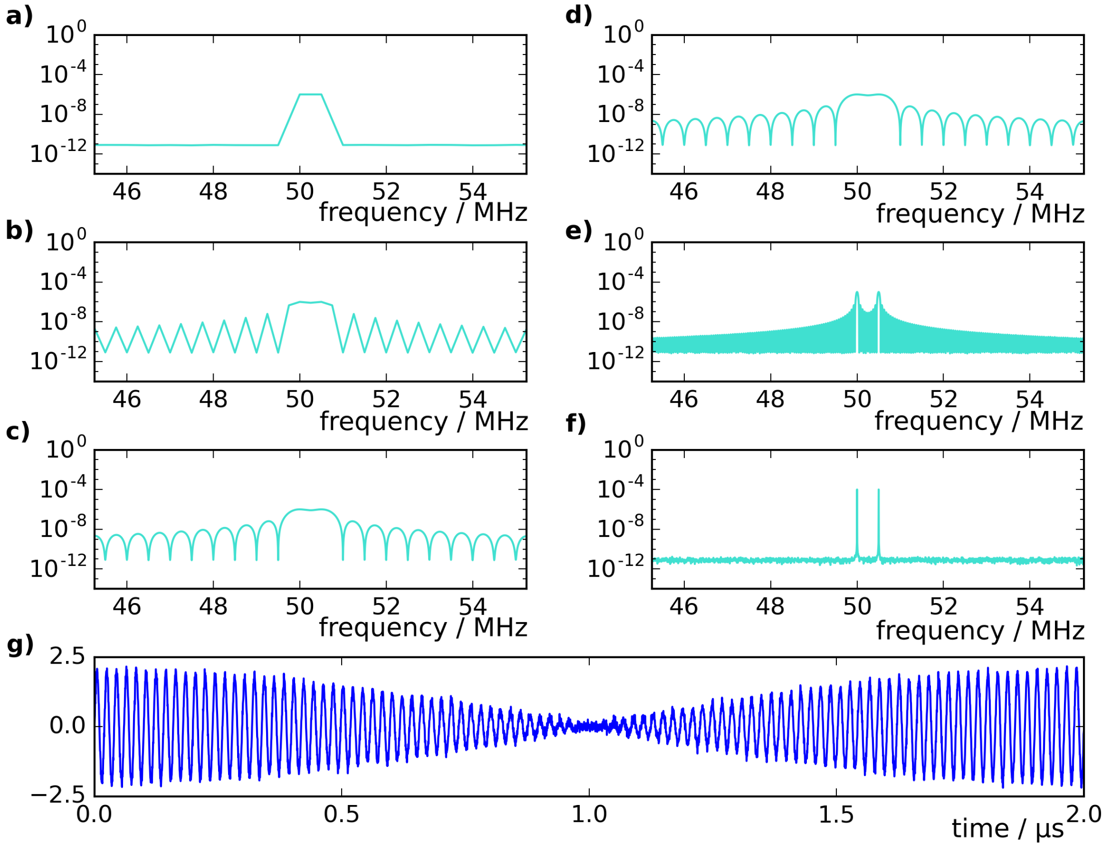

Figure 4.2: A signal consisting of two monochromatic frequencies at 50 MHz and 50.5 MHz is simulated. The influence of zero padding and window length is analyzed. **a)** The window length was set to cover a time span of 2 µs and thus a frequency resolution f_{signal} of 500 kHz is possible. For figures a) and b) zero padding is used to reduce the bin width of the calculated fourier spectrum. The analyzed signal contains 50 % zeros in **b)** and 99 % zeros in **c)**. In **d)** the frequency resolution is again 500 kHz. By increasing the amount of time domain data that is used for calculation of the spectra it is possible to improve the frequency resolution. The frequency resolution is 50 kHz in **e)** and 5 kHz in **f)**. Zero padding is used such that all spectra are calculated with a bin width of 5 kHz. **g)** 2 µs span of the time domain data.

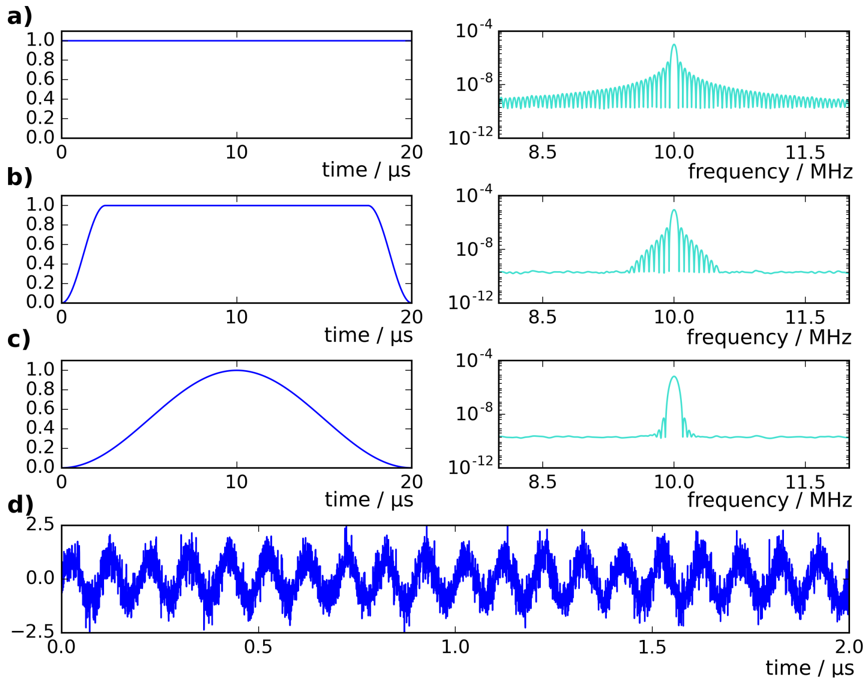

Figure 4.3: A 10 MHz sinusoidal is sampled with 2.5 GS s^{-1} for a window length of 20 µs. Zero padding is used to reduce the fft bin width to 500 Hz. The signal shown in **d)** is analyzed with different window functions. The window function and the calculated spectra are shown. One can see that all windows induce certain features around the expected carrier peak. The decay of these features depends on the choice of the window function as well as the width of the central carrier. **a)** Rectangular window. **b)** Tukey window. **c)** Hann window.

4.2.2 Window function

Let $s(t)$ be the beat signal, $W(t)$ the window function and $F[s](\omega)(t)$ the spectrum of signal $s(t)$ associated with time t. If $W(t)$ is normalized such that $\int_{-\infty}^{\infty} W(t)\, dt = 1$ one can calculate the spectrum according to equation (4.4). For choosing a window function it is important to notice that the calculated spectrum consists of a convolution of the beat fourier spectrum with the fourier spectrum of the window function. This is shown in figure 4.3.

$$F[s](\omega)(t) = \int_{-\infty}^{\infty} s(\tau)W(\tau - t) \exp(-i\omega\tau)\, d\tau \tag{4.4}$$

A monochromatic frequency of 10 MHz was simulated and Gaussian noise with a σ of 50 % the signal amplitude was added. The signal was analyzed with different window functions. The window functions and their corresponding spectra are shown in figure 4.3. The window length is 20 µs in all cases which corresponds to a signal resolution of 50 kHz. Zero padding is used to reach a bin width of 500 Hz. In figure 4.3(a) one can see, that a rectangular window function creates several widely spreading features around the expected carrier. One one hand, the width of this carrier increases when the window function is changed to a Tukey-window (4.3(b)) or a Hann-window (4.3(c)). On the other hand one observes that the amplitude of the features decays faster for such a window. For predicting the form of these features one has to calculate the fourier transformation of the used window function, since the spectrum consists of a convolution of the signal spectrum with the window spectrum.

4.3 Out-of-loop beat spectrum

The out-of-loop beat spectrum between stabilized laser and frequency comb provides information about the lock quality. It is useful in terms of analyzing the stability of a static lock point as well as analyzing certain modulations in frequency or phase of the laser. Firstly the influence of different AOM frequencies is analyzed. Next a frequency modulation is applied to the laser and a proof of concept is given by analyzing the out-of-loop beat spectrum.

4.3.1 mbed noise

As explained in section 2.5 the AOM driving frequency is generated via a VCO which is controlled by an analog line from the mbed microcontroller. Experimentally it turned out that this analog output is disturbed by a 1 kHz noise. The laser follows this noise, since the frequency is smaller that the locking bandwidth. Consequently one can see this kind of low[1] frequency noise on the error signal but not on the in-loop beat spectrum, that is used for stabilization. On the out-of-loop beat spectrum this is nevertheless visible. This is shown in figure 4.4(c). In figure 4.4(a) the out-of-loop beat spectrum is shown over a 2 ms time span. The time resolution is set to 10 µs, which is reasonable since this is a longer time than the inverse control bandwidth. With this a signal resolution of 0.1 MHz is obtained. Exploiting zero padding a bin width of 25 kHz is used. In figure 4.4(a1) the control voltage to the VCO is almost zero which means, that the AOM is driven with 150 MHz. For figures 4.4(a2,a3) the AOM is driven with 200 MHz and 250 MHz, respectively. This corresponds to control voltages of 5 V and 10 V. From the comparison of figures 4.4(a1-a3) one can see that the noise amplitude increases with an increasing output voltage of the VCO control port. The same shaped noise was visible directly on the VCO control port as one can see in figure 4.5. In figure 4.4(b) the maximum of the frequency distribution is shown for each time step. By fitting a constant frequency f_{fit} to this trace it is possible to quantify the amount of noise with the value χ^2, that is defined in equation (4.5).

$$\chi^2 = \sum_i^N (f_i - f_{\text{fit}})^2 \tag{4.5}$$

4.3.2 Lock point jump

The laser frequency should remain constant during the lock point jump. In section 3.3 it has been explained that the error signal was monitored in order to optimize this process. By analyzing the out-of-loop spectrum it is possible to verify the expected stability during this process. The jump process is finished within 3 µs. For a time resolution of $\Delta t = 3$ µs a signal frequency resolution of $\Delta f_{\text{signal}} = 333$ kHz is possible.

4.3.3 Frequency modulation

For this measurement the AOM driving frequency as well as the reference frequency were generated by two function generators which where locked to a 10 MHz signal from an atomic clock. The AOM frequency was set to constant value, while the reference frequency was modulated using another function generator. The amplitude of this modulation was set to 1 MHz and the modulation frequency was chosen to be 5 kHz. The error signal, the in-loop beat signal and the out-of-loop beat signal where recorded

[1] low compared to the locking bandwidth

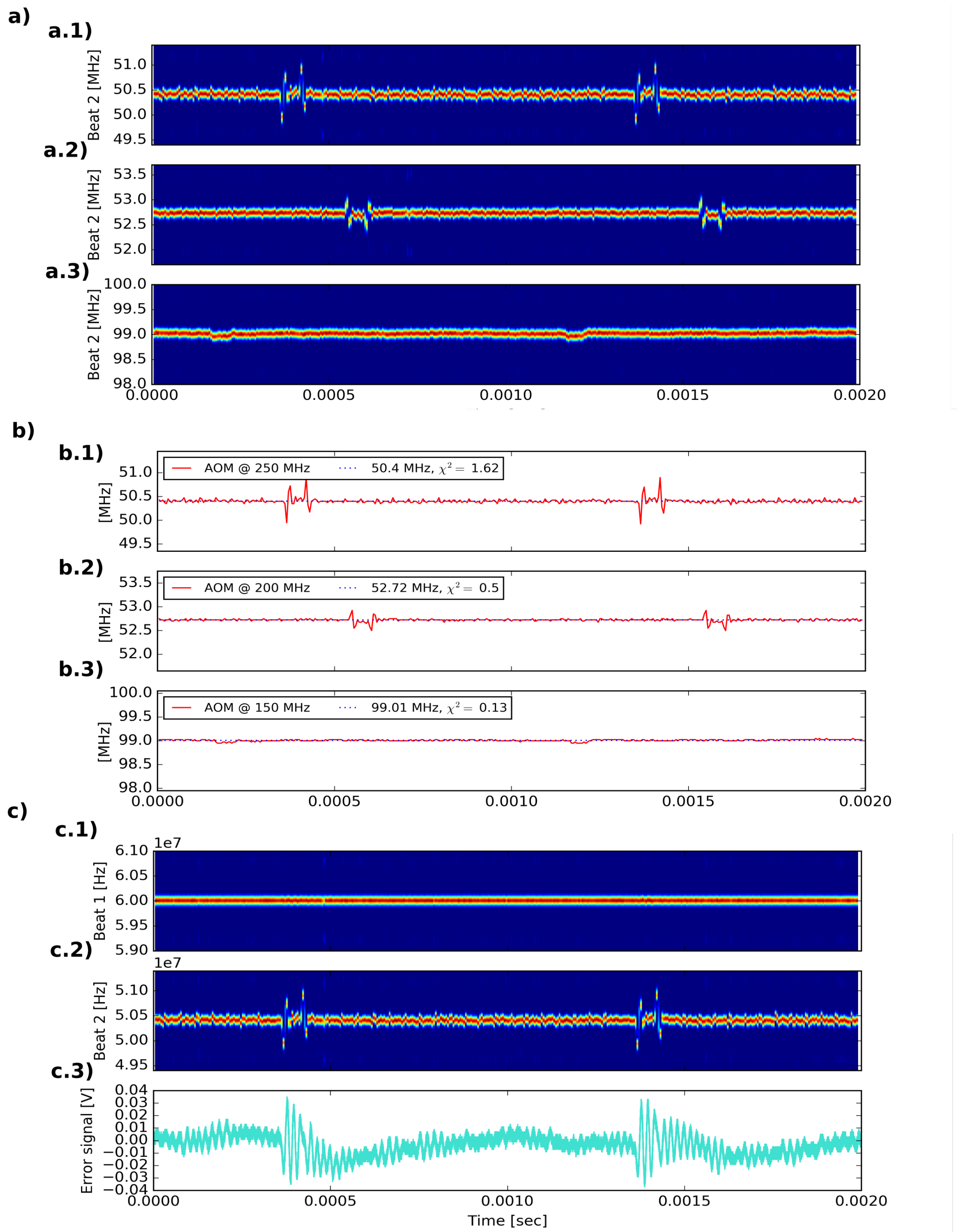

Figure 4.4: **a)** Spectra obtained for different AOM driving frequencies. Due to the noise on the analog control port a effective frequency modulation is applied to the AOM driving frequency. The amplitude of this unintended modulation increases with an increase of the control voltage. In **a.1)** the control voltage is set to 10 V. For **a.2)** and **a.3)** the voltage is set to 5 V and 0.06 V. **b)** The maximum of the spectra from a) is shown. By fitting a constant frequency it is possible to quantify the amount of noise via the χ^2 value. **c)** Due to the unintended frequency modulation the the beat frequency used for stabilizing the laser is also modulated. Since the frequency of this noise is 1 kHz which is lower than the control bandwidth, the feedback corrects these deviations such that the in loop beat frequency remains constant. This causes a modulation of the laser frequency in the experiment arm which is visible in the out of loop spectrum. **c.1)** In loop beat spectrum. **c.2)** Out of loop beat spectrum. **c.3)** Error signal.

with 2.5 GS s^{-1}. Figure 4.7 shows the calculated beat spectra, as well as the recorded error signal. On the in-loop spectrum it is clearly visible that the reference frequency is modulated. On the out of loop spectrum it is clearly visible that the laser frequency follows this modulation. This result proves that a time-frequency analysis of the out-of-loop beat spectrum is useful in terms of analyzing the response of the laser to an applied modulation.

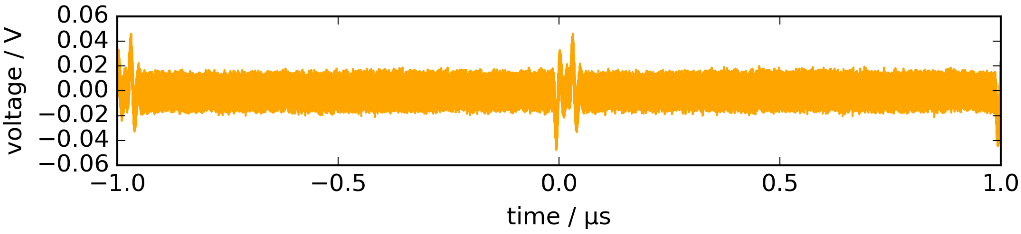

Figure 4.5: The analog output port of the mbed shows a certain noise of frequency 1 kHz. For this measurement the analog output port was connected to an oscilloscope and the AC coupled signal was recorded over 2 ms. The shape of this signal locks very similar to the detected frequency noise analyzed in section 4.3.1.

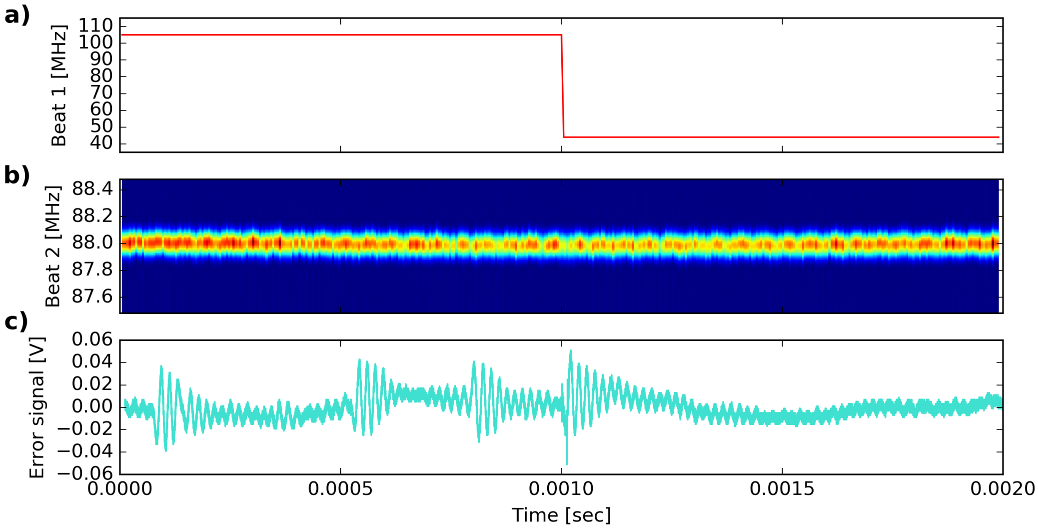

Figure 4.6: **a)** Maximum of the in loop spectrum during the lock point jump. As explained in section 3.3 the reference frequency is changed during the lock point jump. The step from 105 MHz to 44 MHz can be seen. **b)** The spectrum of the out of loop beat signal is shown with a signal frequency resolution of 100 kHz. With this resolution no influence of the lock point jump is visible. **c)** Error signal.

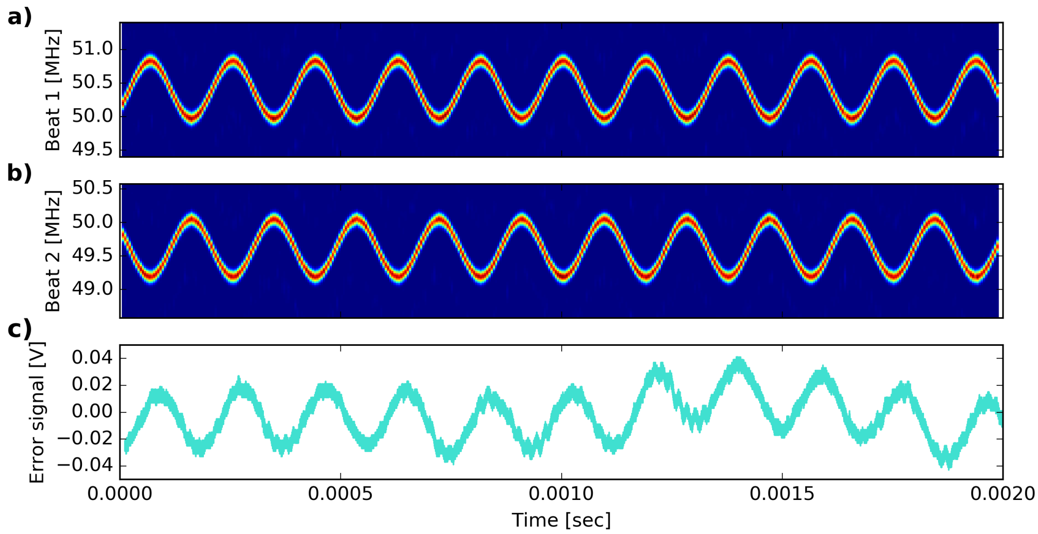

Figure 4.7: For this measurement a frequency modulation was applied to the reference frequency. The amplitude of this modulation was set to 1 MHz and the modulation frequency was sets to 5 kHz. **a)** In loop beat signal. **b)** Out of loop beat signal. **c)** Error signal.

CHAPTER **5**

Summary and Outlook

In this thesis, I presented a phase and frequency lock of an interference filter laser to an optical frequency comb. The stabilization is done by creating a beat signal between both lasers which oscillates with the frequency difference of both laser beams after reasonable low pass filtering (see chapter 2). Since the reference laser is assumed to be stable, fluctuations of the beat frequency and phase are related to corresponding changes of the laser that has to be stabilized. These fluctuations are quantified by a error signal circuit (ESC) [1, 4, 5] which electronically compares the beat signal with a radio frequency provided by a direct digital synthesizer (DDS). The working principle of the ESC is explained as well as the optical and electronic setup used for locking. The working principle of a frequency comb is introduced briefly and difficulties of a lock referenced to an optical frequency comb are pointed out. The frequency components of the beat spectrum are explained and the need for proper electronic filters is derived from that [8].

Scanning the laser frequency continuously over several hundreds of MHz requires scanning across multiple comb lines. This demands eloquent techniques while crossing a comb line in order to maintain phase stability of the lock. In chapter 3 the need of a frequency shifting element is derived from that. Different frequency tuning schemes are explained that make use of the frequency shift by an acusto optical modulator [10, 12]. These schemes allow a continuous tuning of the laser frequency over multiple comb lines and have their own advantages and drawbacks. They have in common that the laser frequency can be tuned by adjusting the reference frequency of the ESC. Hereby, the setpoint for the frequency difference between the laser and the nearest comb line is changed causing a change of the laser frequency by the feedback loop, since the comb spectrum is fixed. The presented schemes differ in terms of the AOM position and the applied driving frequencies. For a continuous scan of the laser frequency it is possible to shift either the light that is used for beat detection [11] or the useful light at the output of the locking setup [10, 12]. In both cases, a change of the respective AOM driving frequency causes a change of the laser frequency. This driving frequency has to be reset at some point, which is denoted as “lock point jump”. During this lock point jump the comb line used for locking changes, while the laser frequency should remain constant. The optimization of this process is explained also in chapter 3. One useful application for the implemented lock scheme is an optical frequency synthesizer [14]. A serial command line interface based on a microcontroller was implemented to set the synthesized optical frequency by automatically generating the necessary control variables for the locking scheme.

In Chapter 4, the analysis of the lock stability is discussed based on a measured spectrum of the “in loop” beat signal. It is obtained that 99.06 % of the power lies inside the central carrier. A locking bandwidth of 1.1 MHz is estimated from the position of the servo bumps. A further analysis obtains the temporal behavior of the “out of loop” beat signal between the stabilized laser and the frequency comb by means of time frequency analysis. This analysis is based on the Fourier transform of the time domain signal which is multiplied by a moving window function [15]. The influence of the window function to the observed spectra as well as the available time resolution Δt and frequency resolution Δf is explained. Both resolutions are not independent since the product is fixed, which can be expressed by $\Delta f \cdot \Delta t = 1$. This analysis approach is finally applied to several out of loop and in loop spectra. Noise generated by the analog output of the mbed microcontroller is precisely quantified and the frequency stability during the lock point jump is verified. In addition a programmed modulation of the laser frequency is verified.

Outlook For this project, the driving frequency for the in loop AOM is generated by a voltage controlled oscillator that is steered by an analog output line of the mbed microcontroller. This output is carrying a 1 kHz noise signal which could not be removed during this project. However, the intrinsic frequency instability of the VCO would limit the lock accuracy even in the absence of control voltage noise. In order to improve the lock stability the corresponding frequency could be generated via a DDS. Such a setup would enable us to optimize the lock point jump further to shorter time scales limited only by the rise time of the AOM instead of the slew rate of the analog mbed output. An additional advantage is, that a frequency step could be send during the lock point jump which is currently impossible due to the limited slew rate. As a consequence the AOM frequency is swept causing a change of the transmitted power during the lock point jump which leads to a saturation of the photo diode amplifiers. This process is explained in more detail in section 3.3. Due to this saturation it is not possible to actively stabilize the laser during the 3 µs jump time.

The investigation of the maximum tuning rate of the laser frequency is of interest in quantum optics experiments. So far tuning rates up to 480 MHz s^{-1} have been demonstrated [8]. The maximum tuning rate could be optimized and compared for the 3 different scanning schemes explained in section 3.2.

In order to analyze not only the frequency stability of the lock, but also the phase stability one could analyze the position of the zero crossings of the out of loop beat signal. By analyzing the time of a zero crossing as function of its number it is possible to interpret the fluctuations around a constant slope as phase noise [16].

For autonomous operation as an optical frequency synthesizer is is of importance to qualify the lock stability in real time by the software on the microcontroller. If indications of multi mode operation of the laser are detected the microcontroller could compensate this via the laser diode current modulation port of the laser controller. Such a second feedback is expected to strongly increase the bandwidth available for frequency tuning.

Bibliography

[1] U. Schünemann et al., *Simple scheme for tunable frequency offset locking of two lasers*, Review of Scientific Instruments **70** (1999) 242, URL: https://doi.org/10.1063/1.1149573 (cit. on pp. 1, 3, 27).

[2] E. D. Black, *An introduction to Pound–Drever–Hall laser frequency stabilization*, American Journal of Physics **69** (2001) 79, URL: https://doi.org/10.1119/1.1286663 (cit. on p. 1).

[3] M. Hohn, *Frequenzstabilisierung eines Diodenlasers mittels Doppler-freier Spektroskopie an einer Erbium-Hohlkathodenlampe (Bachelorarbeit IAP)*, (2017) (cit. on p. 1).

[4] G. Ritt et al., *Laser frequency offset locking using a side of filter technique*, Applied Physics B **79** (2004) 363, URL: https://doi.org/10.1007/s00340-004-1559-6 (cit. on pp. 1, 3, 27).

[5] J. Hughes and C. Fertig, *A widely tunable laser frequency offset lock with digital counting*, Review of Scientific Instruments **79** (2008) 103104, URL: https://doi.org/10.1063/1.2999544 (cit. on pp. 1, 3, 27).

[6] Nobelprize.org., *The Nobel Prize in Physics 2005*, (), Nobel Media AB 2014. Web. 15 Aug 2017., URL: http://www.nobelprize.org/nobel_prizes/physics/laureates/2005/ (cit. on p. 1).

[7] M. S. GmbH, *FC1500-250-ULN User Manual*, (2016) (cit. on p. 4).

[8] L. Ahlheit, *Frequenzvariable Phasenstabilisierung eines Diodenlasers auf einen optischen Frequenzkamm (Bachelorarbeit IAP)*, (2017) (cit. on pp. 5, 6, 14, 27, 28).

[9] *MC100EP140 datasheet*, (2017), URL: https://www.onsemi.com/pub/Collateral/MC100EP140-D.PDF (cit. on p. 8).

[10] T. Sala et al., *Wide-bandwidth phase lock between a CW laser and a frequency comb based on a feed-forward configuration*, Optics Letters **37** (2012) 2592, URL: https://doi.org/10.1364/ol.37.002592 (cit. on pp. 11, 12, 27).

[11] W. Gunton, M. Semczuk and K. W. Madison, *Method for independent and continuous tuning of N lasers phase-locked to the same frequency comb*, Optics Letters **40** (2015) 4372, URL: https://doi.org/10.1364/ol.40.004372 (cit. on pp. 11, 12, 27).

[12] J. D. Jost, J. L. Hall and J. Ye, *Continuously tunable, precise, single frequency optical signal generator*, Opt. Express **10** (2002) 515, URL: http://www.opticsexpress.org/abstract.cfm?URI=oe-10-12-515 (cit. on pp. 11, 12, 27).

[13] T. Fordell et al., *Frequency-comb-referenced tunable diode laser spectroscopy and laser stabilization applied to laser cooling*, Appl. Opt. **53** (2014) 7476, URL: `http://ao.osa.org/abstract.cfm?URI=ao-53-31-7476` (cit. on p. 13).

[14] R. Holzwarth et al., *Optical Frequency Synthesizer for Precision Spectroscopy*, Physical Review Letters **85** (2000) (cit. on pp. 14, 27).

[15] P. D. Welch, *The Use of Fast Fourier Transformation for the Estimation of Power Spectra: A Method Based on Time Averaging Over Short, Modified Periodograms*, IEEE Trans. Audio and Electroacust. **AU-15** (1967) 70 (cit. on p. 28).

[16] M. Schiemangk et al., *Accurate frequency noise measurement of free-running lasers*, Applied Optics **53** (2014) 7138, URL: `https://doi.org/10.1364/ao.53.007138` (cit. on p. 28).